SUPPORTING INFORMATION

Characterization of Chemical Exchange Using Residual Dipolar Coupling

Tatyana I. Igumenova[†], Ulrika Brath[‡], Mikael Akke[‡], and Arthur G. Palmer, III[†,*]

[†]Department of Biochemistry and Molecular Biophysics, Columbia University, New York, New York 10032, USA

[‡]Department of Biophysical Chemistry, Lund University, Box 124, SE-221 00 Lund, Sweden

*Corresponding author. E-mail: agp6@columbia.edu

1. NMR spectroscopy, sample preparation protocol, and characterization of alignment

All NMR experiments were performed using a Bruker Avance NMR spectrometer operating at a ^{1}H Larmor frquency of 500 MHz (125 MHz for ^{13}C) equipped with a 5 mm direct-detect broadband probe. Temperatures were calibrated using methanol and ethylene glycol standard samples[1] and were regulated using the spectrometer VT unit.

Natural abundance N,N-dimethyltrichloroacetamide (DMTCA), CAS registry # 7291-33-0, was purchased from Frinton Laboratories (Vineland, New Jersey) and used without further purification. [^{13}C$_2$-methyl] DMTCA was custom synthesized by Isotec (Miamisburg, OH). Poly-γ-benzyl-L-glutamate (PBLG) with a molecular weight range from 70,000 to 150,000 was purchased from Sigma-Aldrich. To prepare a weakly aligned sample of DMTCA, 190-200 mg of PBLG was dissolved in 600 µl of CDCl$_3$ overnight with continuous mixing and then transferred to the NMR tube. 17 µl of DMTCA was subsequently added to the solution to give a final concentration of 200 mM. The sample was left in the NMR spectrometer magnet overnight to achieve alignment. Isotropic samples of DMTCA were prepared in CDCl$_3$.

Changes in sample alignment with temperature were monitored using the quadrupolar splitting of the ^{2}H nucleus of CDCl$_3$. The temperature dependence of ^{2}H splittings is shown in **Figure S1**. The exquisite sensitivity of ^{2}H splittings to sample temperature has made CDCl$_3$ a useful NMR "thermometer" for nematic liquid crystalline phases[2].

2. Verification of Arrhenius parameters for the conformational exchange process in DMTCA

One-dimensional (1D) ^{1}H NMR spectra were collected as a function of temperature for the natural abundance isotropic sample of DMTCA. Transverse relaxation rate constants, R_2, were calculated using ^{1}H linewidths that were determined using the line fitting routine of the MestReC program. As is evident from **Figure S2**, experimental R_2 values follow the expected temperature dependence calculated using $k = A\exp[-E_a/k_BT]$ with $E_a = 70.13$ kJ/mol, and $A = 1.1\times10^{14}$ s^{-1} as reported by Dimitrov and coworkers[3]. The free-of-exchange transverse relaxation rate constant, R_{20}, was the only adjustable parameter in calculating the fit to the experimental R_2 temperature dependence, and was found to be 4.8 s^{-1}.
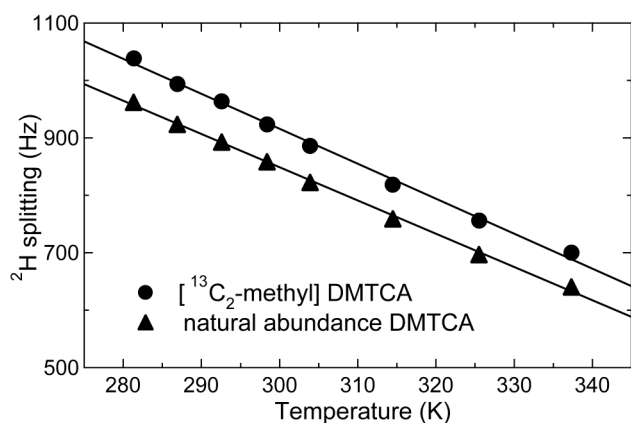
Figure S1. Temperature dependence of ^{2}H quadrupolar splittings of $CDCl_3$ in PBLG/$CDCl_3$ solution.
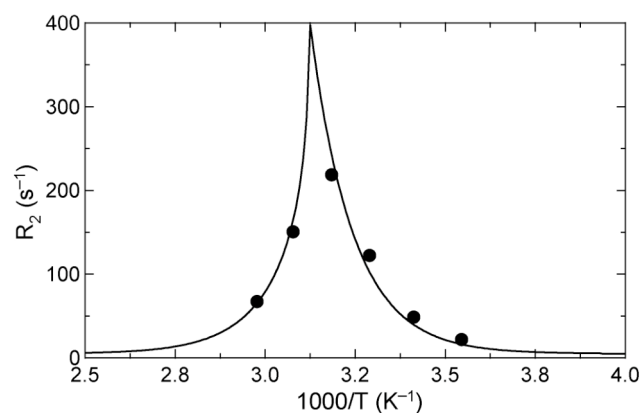
Figure S2. Experimental (circles) and theoretical (line) temperature dependence of ^{1}H transverse relaxation rate constants, calculated using kinetic parameters of Dimitrov and coworkers[3].
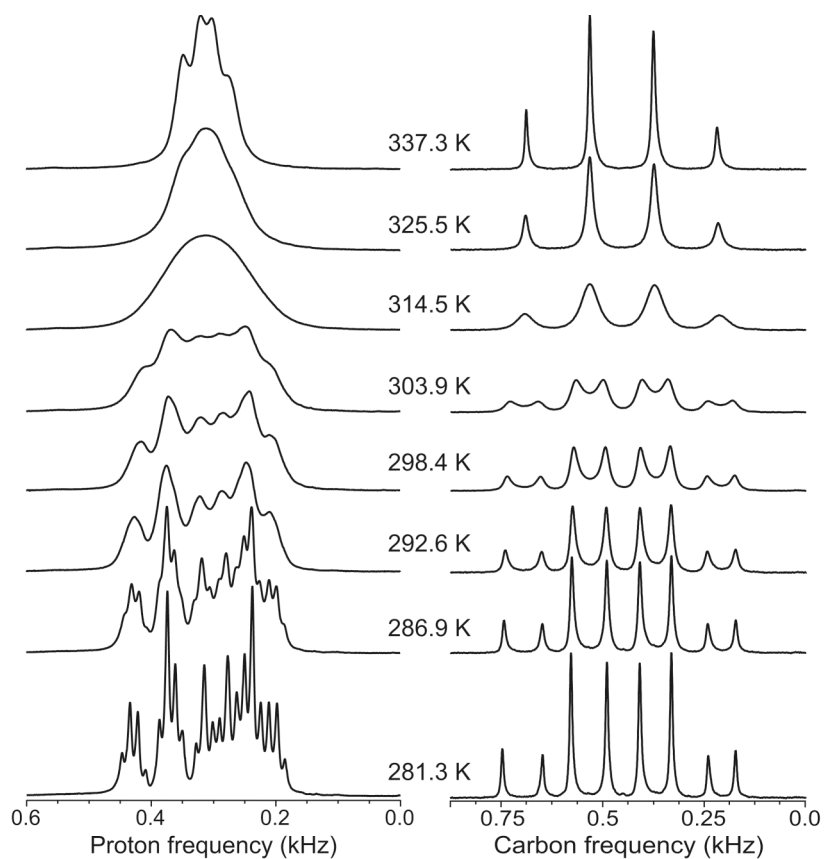

Figure S3. Coupled ^{1}H and ^{13}C NMR spectra collected using weakly aligned natural abundance and [^{13}C$_2$-methyl] DMTCA samples, respectively. The peak intensities of the ^{13}C spectra were adjusted for the number of recorded scans. ^{13}C-^{1}H and ^{1}H-^{1}H RDCs were measured directly using 1D spectra, with peak deconvolution when necessary.

3. ^{1}H and ^{13}C temperature series of the weakly aligned DMTCA

One-dimensional NMR ^{1}H and ^{13}C spectra shown in **Figure S3** were collected using either a single pulse (^{13}C) or Hahn echo (^{1}H) experiments (to eliminate the broad PBLG signals) with recycle delays $> 5T_1$ of the appropriate nucleus. ^{1}H and ^{13}C spectra were collected using natural abundance and [^{13}C$_2$-methyl] DMTCA samples, respectively. The ^{13}C spectrum is weakly ^{1}H-^{13}C coupled at all temperatures. In contrast, the ^{1}H spectrum is weakly ^{1}H-^{1}H coupled, due to intra- and inter-methyl residual dipolar couplings (RDCs), in the slow-exchange limit, but becomes strongly coupled in the fast-exchange limit.

4. Simulations of methyl ^{13}C spectra of DMTCA

To gain insight into the origin of the asymmetry observed for ^{13}C methyl quartets in the slow exchange regime, ^{13}C spectra were simulated using SIMPSON[4]. Each simulation was set up as 7-spin system, with one ^{13}C and six ^{1}H spins. Omitting the second ^{13}C spin was justified by the experimental observation that ^{13}C spectra of the natural abundance DMTCA and [^{13}C$_2$-methyl] DMTCA were identical. The simulations were carried out separately for the upfield and downfield methyl groups. Spin interaction constants were measured from 1D spectra of **Figure S3**, recorded at 281.3 K, and are given in **Table S1.**

Table S1. Spin interaction constants used for SIMPSON simulations

Spin interaction (Hz)	Upfield ^{13}C quartet	Downfield ^{13}C quartet
^{1}H isotropic chemical shift	0.0	128.1
^{13}C isotropic chemical shift	0.0	85.4
^{13}C–^{1}H J coupling	139.4	139.4
^{13}C–^{1}H RDC	10.0	15.4
Intra-methyl ^{1}H–^{1}H RDC	13.1	20.0
Inter-methyl ^{1}H–^{1}H RDC	−6.4	−6.4

500 350 200 50 -100 -250 -400 500 350 200 50 -100 -250 -400
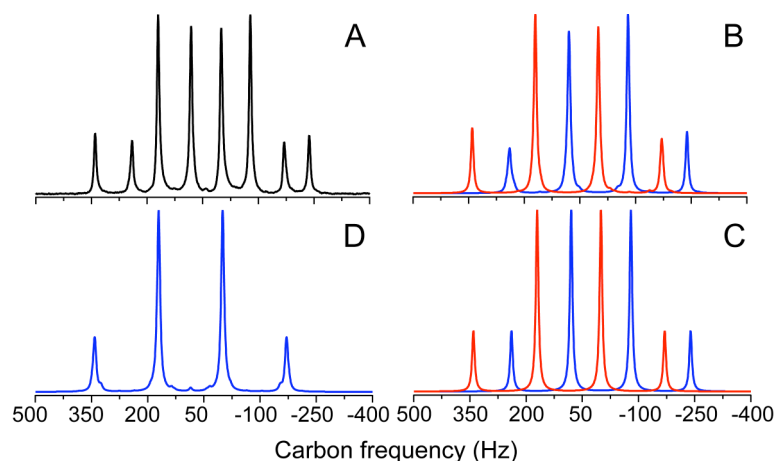
Carbon frequency (Hz)

Figure S4. Experimental (281.3 K) and simulated ^{13}C NMR spectra of methyl groups in DMTCA. The asymmetry of experimentally observed ^{13}C quartets (A) is well reproduced by the simulations (B) and can be eliminated by "turning off" inter-methyl ^{1}H-^{1}H RDCs (C). In contrast to (B), inter-methyl ^{1}H-^{1}H RDCs do not introduce any asymmetry in the ^{13}C spectra in the fast-exchange regime (D).

The results of the simulations (B-D) are compared with the experimental ^{13}C spectrum at 281.3 K (A) in **Figure S4**. When all spin interactions are present, the simulated spectrum (B) shows a quartet intensity pattern similar to that of the experimental data (A). In (C), symmetric quartets for both upfield and downfield methyl groups are recovered by "turning off" inter-methyl ^{1}H-^{1}H RDCs. (D) shows the spectrum of the upfield quartet simulated assuming that all six ^{1}H chemical shifts are degenerate, as would be the case in the fast-exchange limit. The symmetric quartet of (D) indicates that in the fast-exchange regime inter-methyl ^{1}H-^{1}H RDCs do not introduce any asymmetry into the ^{13}C NMR spectra.

5. Temperature gradients and ^{13}C lineshapes

To establish if the temperature gradients in the aligned DMTCA sample influence ^{13}C lineshapes, a series of 1D experiments was recorded with different flow rates of the VT gas. The results are shown in Figure S5 for two temperatures, 292.6 K (A) and 337.3 K (B). The difference spectra between "high" (535 l/h) and "low" (270 l/h and/or 135 l/h) flow rate spectra are shown as inset graphs. Changes in the flow rate, while affecting temperature gradients in the NMR sample[5], do not result in appreciable changes of ^{13}C lineshapes.
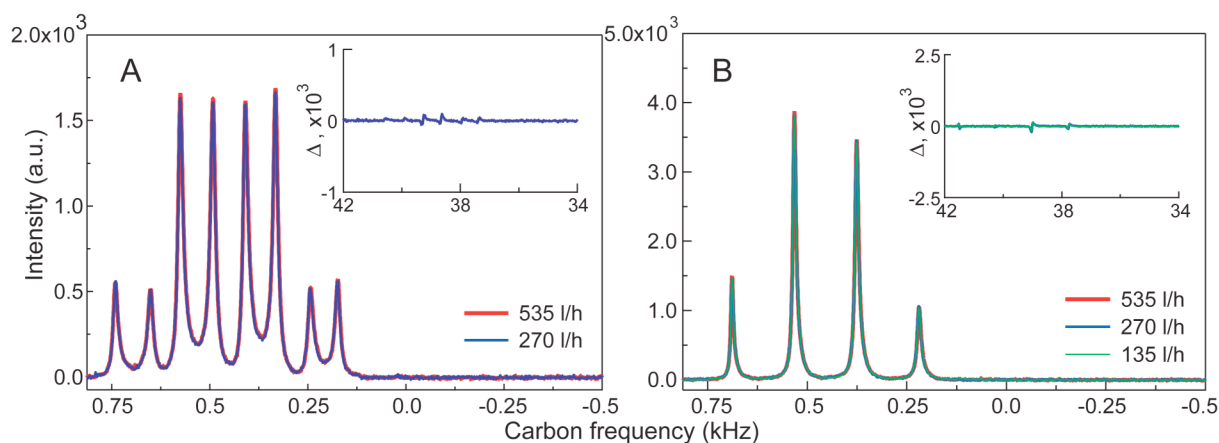

Figure S5. ^{13}C spectra of methyl groups in aligned DMTCA sample collected at 292.6 K (A) and 337.3 K (B). The insets show the difference between "high" (535 l/h) and "low" (270 l/h and/or 135 l/h) flow rate data.

6. Determination of ΔD_{CH} using lineshape analysis

The four components of the methyl ^{13}C 1:3:3:1 quartet are represented by the product operators, $S^+I_1^\alpha I_2^\alpha I_3^\alpha$, $S^+(I_1^\alpha I_2^\alpha I_3^\beta + I_1^\alpha I_2^\beta I_3^\alpha + I_1^\beta I_2^\alpha I_3^\alpha)$, $S^+(I_1^\alpha I_2^\beta I_3^\beta + I_1^\beta I_2^\alpha I_3^\beta + I_1^\beta I_2^\beta I_3^\alpha)$, and $S^+I_1^\beta I_2^\beta I_3^\beta$, in which $S = {}^{13}C$ and I_k is the kth methyl ^{1}H spin. Each quartet component has a unique value $n = n_\alpha - n_\beta$, in which n_α (n_β) are the number of I spins in the α-spin state (β-spin state) The resonance frequency for a quartet component in a single conformational site A is [1]:

$$\omega = \omega_A + n \pi (J_{CH,A} + D_{CH,A}) \tag{S1}$$

in which ω_A is the Larmor frequency, $J_{CH,A}$ is the C-H scalar coupling constant, and $D_{CH,A}$ is the RDC for the ^{13}C spin in site A. A similar equation can be written for site B. In the fast-exchange

regime, the contribution of conformational exchange to the transverse relaxation rate constant of the jth component of the methyl ^{13}C quartet (numbered from 1 to 4 from downfield to upfield for convenience in the present work) is given by [6,7]:

$$R_{ex} = p_A p_B \Delta\omega^2/k_{ex} \qquad (S2)$$

in which p_A and p_B are the site populations of the exchanging conformers, and k_{ex} is the sum of the forward and reverse kinetic rate constants. For DMTCA, $p_A = p_B = 0.5$, and $k_{ex} = 2k$, in which k is the kinetic rate constant for rotation around the amide bond. The difference in resonance frequencies for sites A and B is given by

$$\Delta\omega = \Delta\omega_{iso} + n\pi(\Delta J_{CH} + \Delta D_{CH}) \qquad (S3)$$

in which $\Delta\omega_{iso} = \omega_B - \omega_A$ is the difference in isotropic shifts, $\Delta J_{CH} = J_{CH,B} - J_{CH,A}$, $\Delta D_{CH} = D_{CH,B} - D_{CH,A}$ (taking for convenience site B (A) to represent the downfield (upfield) methyl signal) and n = 3, 1, −1, −3 for the downfield to upfield components of the quartet. For isotropic samples, $\Delta\omega = \Delta\omega_{iso} + n\pi\Delta J_{CH}$. The difference in linewidth between the two outer (component 1 − component 4) or two inner components (component 2 − component 3) of the quartet is given by

$$\Delta\nu_{FWHH} = \Delta R_{20}/\pi + 2|n|\pi\Delta\nu_{iso}(\Delta J_{CH} + \Delta D_{CH})/k_{ex} \qquad (S4)$$

in which ΔR_{20} is the difference between the free-of-exchange transverse relaxation rate constant, $\Delta\nu_{iso} = \Delta\omega_{iso}/2\pi$, and $|n| = 3$ for outer lines $|n| = 1$ for inner lines.

For one-bond [13]C-^{1}H scalar coupling constants, ΔJ_{CH} usually is very small (unless the chemical exchange reaction changes the hybridization of the carbon atom) and in any event can be evaluated using an isotropic sample, in which $\Delta D_{CH} = 0$. The slow-exchange ^{13}C spectrum of DMCTA in the isotropic sample confirms that ΔJ_{CH} is negligible (data not shown); in addition, the identical relaxation dispersion curves obtained for the ^{13}C multiplet components in the isotropic sample also demonstrates that ΔJ_{CH} is negligible in the fast-exchange regime (inset to Figure 2).

The transverse relaxation rate constants may contain contributions from ^{13}C chemical shift anisotropy (CSA)/[1]H-^{13}C dipole and [1]H-^{13}C dipole/[1]H-^{13}C dipole relaxation interference and hence may be different for different components of the quartet. As discussed by Liu and coworkers[8], CSA/dipole relaxation interference contributes primarily to ΔR_{20} for the outer pair or inner pair of resonances. Dipole/dipole relaxation interference contributes to a difference between $R_{20,i}$ for the inner and the outer lines and therefore does not affect the measurement of ΔD_{CH}. The value of the ^{13}C methyl CSA is ~26 ppm and theoretical calculations indicate that CSA/dipole relaxation interference does not contribute significantly to $\Delta\nu_{FWHH}$ for DMTCA. Furthermore, analysis of the ^{13}C spectrum for the isotropic sample of DMTCA showed insignificant differences between the linewidths of the components of the quartet. Thus, ΔD_{CH} was determined from Eq. S4 using $\Delta\nu_{iso}$ and k_{ex} determined for the isotropic DMTCA sample and setting $\Delta J_{CH} = 0$ and $\Delta R_{20} = 0$.

The contribution of ΔR_{20} may become significant for spin systems with larger values of CSA, such as [1]H-^{15}N amide groups in proteins. In such cases, ΔR_{20} can be determined from an isotropic sample, or as discussed below, relaxation dispersion measurements can be used to separate these two contributions to $\Delta\nu_{FWHH}$. Because both CSA/dipole relaxation interference and chemical exchange contribute to multiplet asymmetry, as shown by Eq. S4, experimental methods to measure

relaxation interference in isotropic samples also can be adapted to measure chemical exchange broadening in weakly aligned samples[8].

7. ^{13}C relaxation dispersion analysis

Relaxation dispersion data were recorded at 325.5 K for isotropic and aligned samples of [^{13}C$_2$-methyl] DMTCA using relaxation-compensated[9,10] constant-time[11] 1D ^{13}C-detect CPMG experiments that ensure flat dispersion curves are obtained in the absence of exchange broadening; that is relaxation interference effects that potentially contribute to differences in linewidths for components of the methyl quartet do not contribute to relaxation dispersion. Data were analyzed using the Carver-Richards equation[12]:

$$R_2\left(1/\tau_{cp}\right) = R_{20} + \frac{1}{2}\left(k_{ex} - \frac{1}{\tau_{cp}}\cosh^{-1}\left[D_+\cosh\left(\eta_+\right) - D_-\cos\left(\eta_-\right)\right]\right)$$

(S4)

in which

$$D_\pm = \frac{1}{2}\left[\pm 1 + \frac{\psi + 2\Delta\omega^2}{\left(\psi^2 + \zeta^2\right)^{1/2}}\right]^{1/2}$$

$$\eta_\pm = \frac{\tau_{cp}}{2}\left[\pm\psi + \left(\psi^2 + \zeta^2\right)^{1/2}\right]^{1/2}$$

$$\psi = k_{ex}^2 + \Delta\omega^2$$

$$\zeta = -2\Delta\omega k_{ex}\left(p_A - p_B\right)$$

(S5)

and R_{20} is the effective free-of-exchange transverse relaxation rate constant. Independent fits of the quartet resonances yielded similar results for R_{20} and k_{ex}; accordingly, final optimizations, shown in Figure 2 of the main paper, treated these variables as global parameters. As discussed above, relaxation interference effects make negligible contributions to R_{20} for the different methyl quartet components of DMTCA. Nonlinear fitting was performed using Mathematica (Wolfram). Final optimized parameters are shown in **Table S2**. Results from lineshape analyses and relaxation dispersion measurements using the outer and inner pairs of quartet components are in good agreement and are compared in **Figure S6**.

8. Analysis of intra-methyl ^{1}H-^{1}H RDCs

The multiplet structure for each methyl group in the slow-exchange ^{1}H NMR spectra recorded at 281.3 K (Figure S3) consists of a triplet (intra-methyl ^{1}H-^{1}H RDC) of quartets (inter-methyl ^{1}H-^{1}H RDC). The intra-methyl ^{1}H-^{1}H RDCs obtained by deconvolution of the slow-exchange ^{1}H spectra shown in **Figure S3** are shown in **Figure S7**. These RDCs show the same qualitative trends as functions of temperature as the ^{1}H-^{13}C RDCs (Figure 3 of main paper). The ^{1}H spectrum recorded at 337.3 K in the fast-exchange limit does not show resolved multiplet structure owing to chemical exchange linebroadening. However, this spectrum has the same pattern of asymmetry as the corresponding ^{13}C NMR spectrum, confirming that the difference in intra-methyl RDCs is negative at this temperature as predicted by the extrapolated linear fits in **Figure S7**.

Simulations confirm that the spectrum is expected to be symmetric if $\Delta D_{HH,intra} = 0$. The linear correlation between ^1H-^1H and ^1H-^{13}C RDCs is exhibited in **Figure S7**; the slope of 2.1 matches theoretical predictions[13].

Table S2. Conformational exchange parameters for isotropic and aligned DMTCA

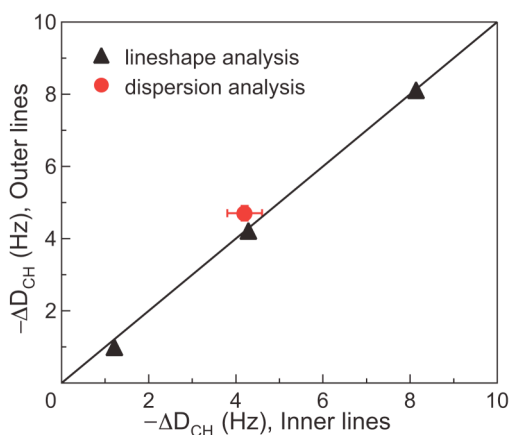|	R_{20}, s^{-1}	k_{ex}, s^{-1}	$\Delta\omega/2\pi$, Hz
Isotropic DMTCA			
	0.70 ± 0.02	1351 ± 3	76.6 ± 0.1
Aligned DMTCA			
Outer 1	2.38 ± 0.08	1300 ± 12	70.0 ± 0.5
Inner 2			73.4 ± 0.3
Inner 3			77.6 ± 0.3
Outer 4			84.1 ± 0.3

Figure S6. Differences in ^1H-^{13}C RDCs for downfield and upfield methyl resonances as determined from the inner and outer pairs of multiplet components in the fast-exchange regime (T > 312 K) using lineshape analysis or relaxation dispersion measurements.
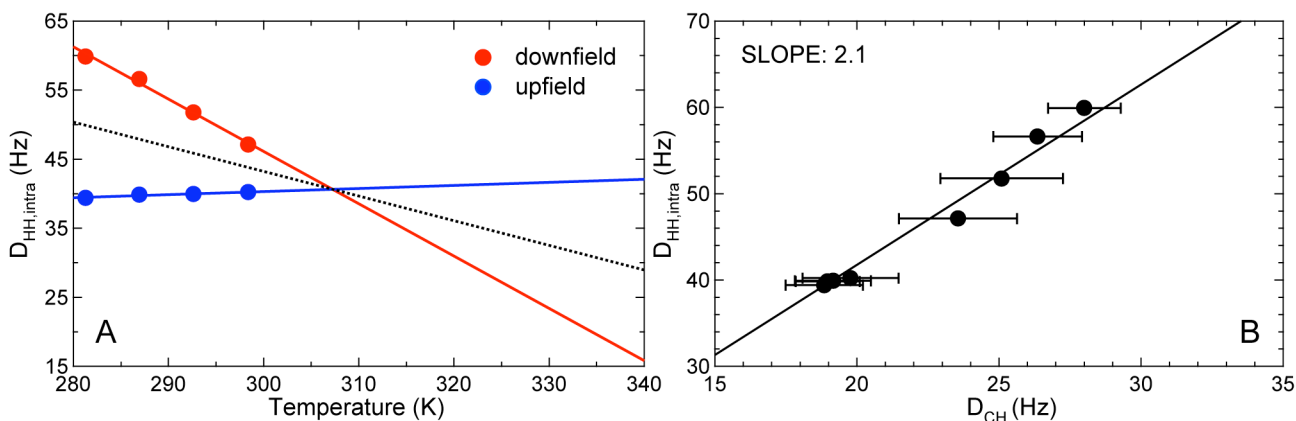
Figure S7. (A) Temperature dependence of intra-methyl ^{1}H-^{1}H RDCs obtained from deconvolution of the slow-exchange ^{1}H spectra for T < 300 K in Figure S3. (B) Comparison of intra-methyl ^{1}H-^{1}H and ^{1}H-^{13}C RDCs.

References

1.   Cavanagh, J.; Fairbrother, W. J.; Palmer, A. G.; Rance, M.; Skelton, N. J., Protein NMR Spectroscopy: Principles and Practice. Academic Press: Amsterdam, 2007; p 1-885.
2.   Vold, R. L.; Vold, R. R., J. Magn. Reson. 1983, 55, 78-87.
3.   Dimitrov, V. S.; Ladd, J. A., Magn. Reson. Chem. 1985, 23, 529-532.
4.   Bak, M.; Rasmussen, J. T.; Nielsen, N. C., J. Magn. Reson. 2000, 147, 296-330.
5.   Loening, N. M.; Keeler, J., J. Magn. Reson. 2002, 159, 55-61.
6.   Kaplan, J. I.; Fraenkel, G., NMR of Chemically Exchanging Systems. Academic Press: New York, 1980; p 1-165.
7.   Luz, Z., In Nuclear Magnetic Resonance of Liquid Crystals, Emsley, J. W., Ed. D. Reidel Publishing Company: Dordrecht, Holland, 1983; Vol. 141, pp 315-340.
8.   Liu, W. D.; Zheng, Y.; Cistola, D. P.; Yang, D. W., J. Biomol. NMR 2003, 27, 351-364.
9.   Loria, J. P.; Rance, M.; Palmer, A. G., J. Am. Chem. Soc. 1999, 121, 2331-2332.
10. Loria, J. P.; Rance, M.; Palmer, A. G., J. Biomol. NMR 1999, 15, 151-155.
11. Skrynnikov, N. R.; Mulder, F. A. A.; Hon, B.; Dahlquist, F. W.; Kay, L. E., J. Am. Chem. Soc. 2001, 123, 4556-4566.
12. Carver, J. P.; Richards, R. E., J. Magn. Reson. 1972, 6, 89-105.
13. Kaikkonen, A.; Otting, G., J. Am. Chem. Soc. 2001, 123, 1770-1771.